Aircraft Attitude Determination Algorithms Employing Gravity Vector Estimations and Velocity Measurements

Raúl de Celis and Luis Cadarso
European Institute for Aviation Training and Accreditation (EIATA), Rey Juan Carlos University, 28943 Fuenlabrada, Madrid, Spain

Keywords: IMU, GNSS, Attitude Determination, Sensor Model, Projectile, Terminal Guidance.

Abstract: Precision on Navigation, Guidance and Control of aircraft is dependent on the precision of the measurement system both for position and attitude. It is well known in aerospace engineering that the rotation of an aircraft or space vehicle can be determined measuring two vectors in two different reference systems. Velocity vector in an aerospace vehicle can be determined in an inertial reference frame directly from a GNSS-based sensor. Also this velocity vector can be determined by integrating the acceleration measurements in an aircraft body fixed reference frame. By estimating gravity vector in an inertial reference frame, which currently is perfectly tabulated, and in a body reference frame, and combining these measurements with the velocity vector, rotation of the body can be determined. Application of these concepts is especially interesting in order to substitute high-precision attitude determination devices, which are usually expensive as they are forced to bear high solicitations as for instance G forces.

1 INTRODUCTION

Obtaining precise attitude information is essential for navigation and control. The effectiveness of navigation and control is determined by the degree of precision of the navigation and control systems, including inertial measurement units (Ma et al., 2011). There is an extensive body of literature regarding attitude estimation using various sensor inputs (Crassidis et al., 2007).

Traditionally, in order to obtain accurate values for determining attitude, expensive and/or weighty units, such as as laser or fiber optic gyroscopes and accelerometers, or their MEMS equivalents, must be employed. High-performance electro-static gyroscopes require expensive vacuum-packaging, to maintain the high-Q of the MEMS (Ismail et al., 2015). Moreover, when high-demanding maneuvers are performed this equipment may become extremely expensive.

It is well-known that the attitude of an aerovehicle can be determined by integrating the angular rates (pitch, roll, and yaw rates) of the vehicle. Nevertheless, accuracy requirements usually cannot be satisfied by using the inexpensive sensors (Ma et al., 2011). This problem becomes even more important when the vehicle cannot be reused: low-cost attitude determination systems are of key importance for these applications. For example, (Gebre-Egziabher et al., 2000) describe an attitude determination system that is based on two vector measurements of non-zero, non-co-linear vectors. Using the Earth's magnetic field and gravity as the two measured quantities, a low-cost attitude determination system is proposed. (Gebre-Egziabher et al., 1998) develop an inexpensive Attitude Heading Reference System for general aviation applications by fusing low cost automotive grade inertial sensors with GPS. The inertial sensor suit consists of three orthogonally mounted solid state rate gyros. (Eure et al., 2013) describe an attitude estimation algorithm derived by post-processing data from a small low cost Inertial Navigation System recorded during the flight of a sub-scale commercial off the shelf UAV. Estimates of the UAV attitude are based on MEMS gyro, magnetometer, accelerometer, and pitot tube inputs. (Henkel and Iafrancesco, 2014) state that low-cost GNSS receivers and antennas can provide a precise attitude and drift-free position information, but accuracy is not continuous. Inertial sensors are robust to GNSS signal interruption and very precise over short time frames, which enables a reliable cycle slip correction, but low-cost inertial sensors suffer from a substantial drift. The authors propose a tightly coupled position and attitude determination method for two low-cost GNSS receivers, a gyroscope and an accelerometer and obtain a heading

Celis, R. and Cadarso, L.
Aircraft Attitude Determination Algorithms Employing Gravity Vector Estimations and Velocity Measurements.
DOI: 10.5220/0006393203770385
In *Proceedings of the 14th International Conference on Informatics in Control, Automation and Robotics (ICINCO 2017) - Volume 1*, pages 377-385
ISBN: 978-989-758-263-9

with an accuracy of 0.25°/baseline length [m] and an absolute position with an accuracy of 1 m. Similar developments may be found within space vehicles, for example in (Springmann and Cutler, 2014).

However, as stated in (Yun et al., 2008), many of the presented methods such as the ones employing local magnetic field vectors, are only valid for estimating the orientation of a static or slow-moving rigid body. In the research described in this paper, two measured quantities are used to obtain attitude information for high dynamic vehicles: speed and gravity vectors. They are obtained in two different reference frames using a GNSS sensor and a strap-down accelerometer.

1.1 Contributions

The main contribution of this paper is the development of a novel algorithm which aims at avoiding the use of gyroscopes, and its implicit high costs if high precision is required (Ismail et al., 2015), in a long term and to require lower performance gyroscopes for attitude determination in the immediate term. This is pretended to decrease costs in attitude sensors and even to improve attitude determination by applying filtering techniques, especially for artillery device purposes, where high solicitation force conditions increase the price of precise attitude determination devices such as gyroscopes.

Nonlinear simulations based on ballistic rocket launches are performed to determine real attitude and compare it to the estimated attitude obtained from the algorithms. The applicability of the proposed solution for aircraft flight navigation, guidance and control, and for ballistic rocket terminal guidance, where attack and side-slip aerodynamic angles are relatively small, is also demonstrated.

This paper is organized as follows. Section II describes the problem in detail. Section III is devoted to flight dynamics and sensor models. Section IV shows simulations results. Finally, in Section V some conclusions and further work are drawn.

2 PROBLEM DESCRIPTION

Attitude determination is a fundamental field in aerospace engineering, as maneuvers in order to change vehicle trajectories are governed by aerodynamic forces, which depend directly on ship orientation angles. Furthermore, attitude in artillery rockets terminal phase is vital as it determines factors such as penetrability of payload or countermeasures avoidability. Therefore, developing algorithms to improve attitude determination is a cornerstone in guidance, navigation and control research.

One of the techniques to determine attitude is to calculate it from the director cosine matrix (DCM) which completely determines the rotation of a body. Two reference frames are defined, one fixed to the body and another one as a reference. In order to obtain the DCM, a geometrical plane defined in both reference triads must be obtained. Every geometrical plane is defined by two vectors. Therefore, knowing the same two vectors expressed in the two reference frames, the DCM can be calculated.

2.1 Triad Definition

Two axes systems are defined in order to express forces and moments: North-East-Down (NED) axes and Body (B) axes. NED axes are defined by sub index NED. x_{NED} pointing north, z_{NED} perpendicular to x_{NED} and pointing nadir, and y_{NED} forming a clockwise trihedron. Body axes are defined by sub index B. x_B pointing forward and contained in the plane of symmetry of the aircraft, z_B perpendicular to x_B pointing down and contained in the plane of symmetry of the aircraft, and y_B forming a clockwise trihedron. The origin of body axes is located at the center of mass of the aircraft.

2.2 Involved Vectors Determination

If a GNSS sensor device is equipped on the aircraft, velocity vector can be directly expressed from sensor measurements in the NED triad. Expression for velocity in NED is defined on equation (1), where $v_{x_{NED}}, v_{y_{NED}}$ and $v_{z_{NED}}$ are the components of this velocity vector in NED axes.

$$\overrightarrow{v_{NED}} = [v_{x_{NED}}, v_{y_{NED}}, v_{z_{NED}}]^T \quad (1)$$

The same velocity vector expressed in body triad can be obtained from a set of accelerometers equipped on the ship, one on each of the axes. This devices are able to measure acceleration. After integration of each of the components along the time, velocity vector is obtained as it is expressed on equation (2), where a_{x_B}, a_{y_B} and a_{z_B} are the components of the acceleration vector in body axes.

$$\overrightarrow{v_B} = \int [a_{x_B}, a_{y_B}, a_{z_B}]^T dt \quad (2)$$

Another vector expressed in the two reference frames is required in order to define the rotation. Gravity vector is easily determined in NED triad as

it always points to z_{NED}, as it is shown on equation (3). g is the gravity acceleration modulus that in this model is a fixed constant of value $9.81 m/s^2$. For more complicated models it may be modeled depending on the latitude and longitude of the aircraft.

$$\overrightarrow{g_{NED}} = g[0,0,1]^T \tag{3}$$

The keystone of the presented attitude determination method is determining gravity vector in body axes. Rudimentary inertial measurement units are able to determine this gravity vector in order to subtract it from measured acceleration and provide better results for position and velocity calculations in body axes. The methods to calculate this gravity vector are well developed in (Mizell, 2003). For example by determining the continuous component of the measured acceleration employing a low pass filter as it is indicated on equations 4 and 5, on where Jerk on body axes is calculated by the derivation of acceleration and after that integrated in order to obtain non-continuous component of acceleration, then, by subtracting this non-continuous component to the measured acceleration, gravity vector is estimated.

$$\overrightarrow{Jerk_B} = \frac{d}{dt}[a_{x_B}, a_{y_B}, a_{z_B}]^T \tag{4}$$

$$\overrightarrow{g_B} = [a_{x_B}, a_{y_B}, a_{z_B}]^T - \int \overrightarrow{Jerk_B} dt \tag{5}$$

Another method to obtain gravity vector is by integrating the mechanization equations (Savage, 2000) and manipulate consequently the resulting equations. In this paper it is assumed that gravity vector in body axes is provided directly by the inertial sensor, with its associated error. It is defined in equation (6), where g_{x_B}, g_{y_B} and g_{z_B} are gravity vector components expressed in body axes.

$$\overrightarrow{g_B} = [g_{x_B}, g_{y_B}, g_{z_B}]^T \tag{6}$$

3 ATTITUDE DETERMINATION ALGORITHM

In order to simplify the calculus, an orthonormal base must be defined in both axes systems, B and NED. This orthonormal base is defined by unitary vectors $\vec{i}, \vec{j}$ and $\vec{k}$ expressed in both bases and defined by expressions (7), (8), (9), (10), (11) and (12).

$$\overrightarrow{i_{NED}} = \frac{\overrightarrow{v_{NED}}}{\|\overrightarrow{v_{NED}}\|} \tag{7}$$

$$\overrightarrow{j_{NED}} = \frac{\overrightarrow{v_{NED}} \times \overrightarrow{g_{NED}}}{\|\overrightarrow{v_{NED}} \times \overrightarrow{g_{NED}}\|} \tag{8}$$

$$\overrightarrow{k_{NED}} = \frac{\overrightarrow{i_{NED}} \times \overrightarrow{j_{NED}}}{\left\|\overrightarrow{i_{NED}} \times \overrightarrow{j_{NED}}\right\|} \tag{9}$$

$$\overrightarrow{i_B} = \frac{\overrightarrow{v_B}}{\|\overrightarrow{v_B}\|} \tag{10}$$

$$\overrightarrow{j_B} = \frac{\overrightarrow{v_B} \times \overrightarrow{g_B}}{\|\overrightarrow{v_B} \times \overrightarrow{g_B}\|} \tag{11}$$

$$\overrightarrow{k_B} = \frac{\overrightarrow{i_B} \times \overrightarrow{j_B}}{\left\|\overrightarrow{i_B} \times \overrightarrow{j_B}\right\|} \tag{12}$$

After defining an orthonormal base in the two systems of axes, the expression to determine the DCM is indicated on (13), where $\left[\overrightarrow{i_B}, \overrightarrow{j_B}, \overrightarrow{k_B}\right]$ is a $3x3$ square matrix composed of orthonormal vectors in body triad, $\left[\overrightarrow{i_{NED}}, \overrightarrow{j_{NED}}, \overrightarrow{k_{NED}}\right]$ express the same concept in NED triad, and $DCM_{B,NED}$ is the director cosine matrix that transforms NED triad into body triad.

$$\left[\overrightarrow{i_B}, \overrightarrow{j_B}, \overrightarrow{k_B}\right] = DCM_{B,NED} \left[\overrightarrow{i_{NED}}, \overrightarrow{j_{NED}}, \overrightarrow{k_{NED}}\right] \tag{13}$$

The DCM matrix can be solved from (13) as it is shown in (14). Note that employing an orthonormal base simplifies the calculation of the inverse matrix as it is the transposed matrix.

After obtaining the director cosine matrix, the rotation must be characterized. The most suitable method to express this rotation is through quaternions, as they avoid any possible singularities on the poles of rotation (Kuipers et al., 1999). The matrix equation that relates $DCM_{B,NED}$ and quaternions is showed in (15), where q_i for $i = \{0,3\}$, are the quaternions, and $M_{j,k}$ for $j = \{1,3\}$ and $k = \{1,3\}$ are the DCM matrix coefficients.

The expressions in (16), (17), (18) and (19) may be used in order to solve quaternions.

$$DCM_{B,NED} = \left[\overrightarrow{i_B}, \overrightarrow{j_B}, \overrightarrow{k_B}\right] \left[\overrightarrow{i_{NED}}, \overrightarrow{j_{NED}}, \overrightarrow{k_{NED}}\right]^{-1} = \left[\overrightarrow{i_B}, \overrightarrow{j_B}, \overrightarrow{k_B}\right] \left[\overrightarrow{i_{NED}}, \overrightarrow{j_{NED}}, \overrightarrow{k_{NED}}\right]^T \tag{14}$$

$$DCM_{B,NED} = \begin{bmatrix} M_{1,1} & M_{1,2} & M_{1,3} \\ M_{2,1} & M_{2,2} & M_{2,3} \\ M_{3,1} & M_{3,2} & M_{3,3} \end{bmatrix} = \begin{bmatrix} q_0^2+q_1^2-q_2^2-q_3^2 & 2(q_1q_2+q_0q_3) & 2(q_1q_3-q_0q_2) \\ 2(q_1q_2-q_0q_3) & q_0^2-q_1^2+q_2^2-q_3^2 & 2(q_2q_3+q_0q_1) \\ 2(q_1q_3+q_0q_2) & 2(q_2q_3-q_0q_1) & q_0^2-q_1^2-q_2^2+q_3^2 \end{bmatrix} \tag{15}$$

$$q_0 = \begin{cases} \frac{1}{2}\sqrt{1+Tr} \text{ if } Tr > 0 \\ \frac{1}{2}C_1(M_{2,3}-M_{3,2}) \text{ if } Tr \leq 0 \text{ and } M_{1,1} \geq M_{2,2} \text{ and } M_{1,1} \geq M_{3,3} \\ \frac{1}{2}C_2(M_{3,1}-M_{1,3}) \text{ if } Tr \leq 0 \text{ and } M_{2,2} > M_{1,1} \text{ and } M_{2,2} > M_{3,3} \\ \frac{1}{2}C_3(M_{1,2}-M_{2,1}) \text{ if } Tr \leq 0 \text{ and } M_{3,3} > M_{2,2} \text{ and } M_{3,3} > M_{1,1} \end{cases} \quad (16)$$

$$q_1 = \begin{cases} \frac{1}{2}C_0(M_{2,3}-M_{3,2}) \text{ if } Tr > 0 \\ \frac{1}{2}\sqrt{1+M_{1,1}-M_{2,2}-M_{3,3}} \text{ if } Tr \leq 0 \text{ and } M_{1,1} \geq M_{2,2} \text{ and } M_{1,1} \geq M_{3,3} \\ \frac{1}{2}C_2(M_{1,2}+M_{2,1}) \text{ if } Tr \leq 0 \text{ and } M_{2,2} > M_{1,1} \text{ and } M_{2,2} > M_{3,3} \\ \frac{1}{2}C_3(M_{3,1}+M_{1,3}) \text{ if } Tr \leq 0 \text{ and } M_{3,3} > M_{2,2} \text{ and } M_{3,3} > M_{1,1} \end{cases} \quad (17)$$

$$q_2 = \begin{cases} \frac{1}{2}C_0(M_{3,1}-M_{1,3}) \text{ if } Tr > 0 \\ \frac{1}{2}C_1(M_{1,2}+M_{2,1}) \text{ if } Tr \leq 0 \text{ and } M_{1,1} \geq M_{2,2} \text{ and } M_{1,1} \geq M_{3,3} \\ \frac{1}{2}\sqrt{1+M_{2,2}-M_{1,1}-M_{3,3}} \text{ if } Tr \leq 0 \text{ and } M_{2,2} > M_{1,1} \text{ and } M_{2,2} > M_{3,3} \\ \frac{1}{2}C_3(M_{2,3}+M_{3,2}) \text{ if } Tr \leq 0 \text{ and } M_{3,3} > M_{2,2} \text{ and } M_{3,3} > M_{1,1} \end{cases} \quad (18)$$

$$q_3 = \begin{cases} \frac{1}{2}C_0(M_{1,2}-M_{2,1}) \text{ if } Tr > 0 \\ \frac{1}{2}C_1(M_{3,1}+M_{1,3}) \text{ if } Tr \leq 0 \text{ and } M_{1,1} \geq M_{2,2} \text{ and } M_{1,1} \geq M_{3,3} \\ \frac{1}{2}C_2(M_{2,3}+M_{3,2}) \text{ if } Tr \leq 0 \text{ and } M_{2,2} > M_{1,1} \text{ and } M_{2,2} > M_{3,3} \\ \frac{1}{2}\sqrt{1+M_{3,3}-M_{1,1}-M_{2,2}} \text{ if } Tr \leq 0 \text{ and } M_{3,3} > M_{2,2} \text{ and } M_{3,3} > M_{1,1} \end{cases} \quad (19)$$

where, Tr, C_0, C_1, C_2 and C_3 are defined by (20), (21), (22), (23), and (24), respectively.

$$Tr = M_{1,1} + M_{2,2} + M_{3,3} \quad (20)$$

$$C_0 = \begin{cases} \frac{1}{\sqrt{1+Tr}} \text{ if } \sqrt{1+Tr} > 0 \\ 0 \text{ else} \end{cases} \quad (21)$$

$$C_1 = \begin{cases} \frac{1}{\sqrt{1+M_{1,1}-M_{2,2}-M_{3,3}}} \text{ if } \sqrt{1+M_{1,1}-M_{2,2}-M_{3,3}} > 0 \\ 0 \text{ else} \end{cases} \quad (22)$$

$$C_2 = \begin{cases} \frac{1}{\sqrt{1+M_{2,2}-M_{1,1}-M_{3,3}}} \text{ if } \sqrt{1+M_{2,2}-M_{1,1}-M_{3,3}} > 0 \\ 0 \text{ else} \end{cases} \quad (23)$$

$$C_3 = \begin{cases} \frac{1}{\sqrt{1+M_{3,3}-M_{1,1}-M_{2,2}}} \text{ if } \sqrt{1+M_{3,3}-M_{1,1}-M_{2,2}} > 0 \\ 0 \text{ else} \end{cases} \quad (24)$$

It is known that quaternions themselves are enough to express rotations without singularities, but it is also known than conceptually they are difficult to be visualized. An easier manner to define these rotations is by means of Euler angles. Concretely, the most common aeronautical rotation is defined by roll (ϕ), pitch (θ), and yaw (ψ) angles. The expressions that relate quaternions with Euler angles are defined by (25), (26) and (27).

$$\phi = atan2[2(q_2q_3 + q_0q_1), q_0^2 - q_1^2 - q_2^2 + q_3^2] \quad (25)$$

$$\theta = asin[-2(q_1q_3 - q_0q_2)] \quad (26)$$

$$\psi = atan2[2(q_1q_2 + q_0q_3), q_0^2 + q_1^2 - q_2^2 - q_3^2] \quad (27)$$

These Euler angles obtained from measurements may be used to characterize rotations and angular speeds in navigation guidance and control algorithms.

4 FLIGHT DYNAMICS AND SENSOR MODEL

The flight dynamics model in (de Celis et al., 2017) is employed. The equations of motion are integrated using a fixed time step RungeKutta scheme of fourth order to obtain a single flight trajectory. A set of ballistic simulated shots, with no wind perturbations, is performed varying shot angle from 15° to 75° taking 1° steps, and also varying initial azimuth angle from 0° to 360° taking 45° steps. An example of these trajectories for a shot angle of 45° and for the whole set of azimuths is shown in Figure 1.

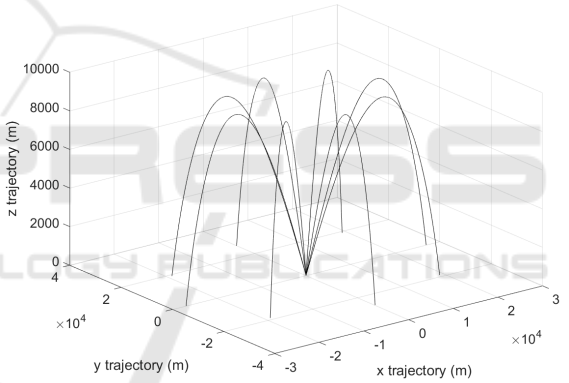

Figure 1: Trajectories for 45° on initial pitch shot angle and 8 different azimuths.

GNSS sensors are modeled adding a white noise of null average and maximum absolute values of $m_p = 3m$ and of $m_v = 0.01m/s$ for position and velocity, respectively, to the simulated values obtained from model.

Accelerometers are modeled as second order systems, with a natural frequency of 300 Hz and a damping factor of 0.7. A white noise of null average and maximum absolute value of $m_a = 10^{-6}m/s^2$ and a bias of $10^{-6}m/s^2$ is added. Note that accelerometers will provide both acceleration in body axes, which will be employed on the determination of velocity vector in body axes, and gravity vector in body axes.

The modeling of the sensors has been based on relatively low-cost equipment. This fact will induce significant errors on measurements, which will determine the suitability of the attitude calculation method.

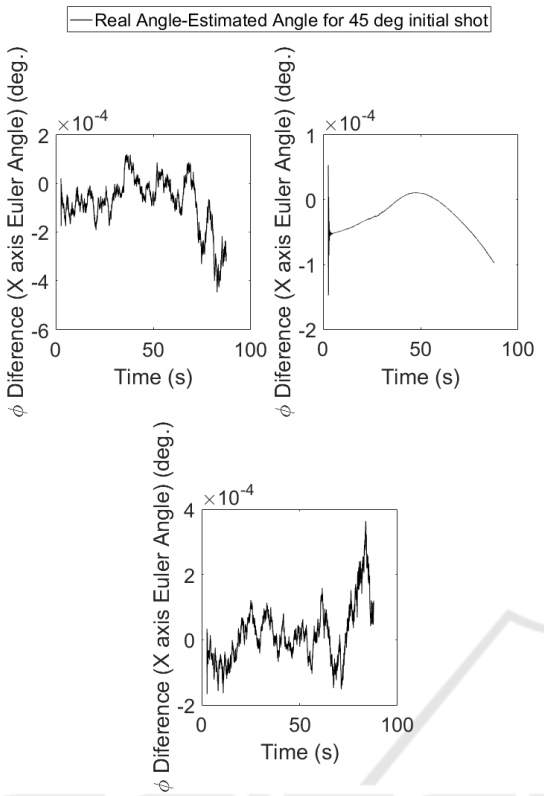

Figure 2: Comparison between estimated and real magnitudes for aircraft roll angle (ϕ) for a shot angle of 45 deg. and azimuths of 0° (left), 45° (right) and 90° (bottom).

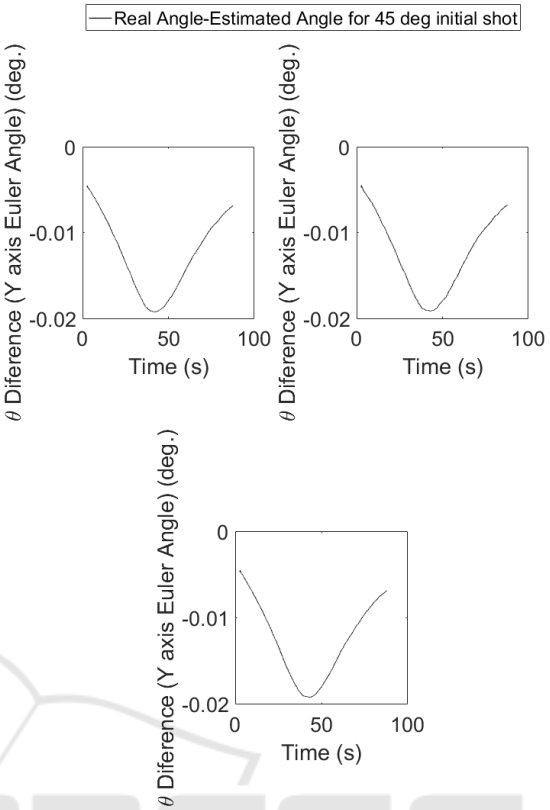

Figure 3: Comparison between estimated and real magnitudes for aircraft pitch angle (θ) for a shot angle of 45 deg. and azimuths of 0° (left), 45° (right) and 90° (bottom).

However, as it is shown in the following section, the results are accurate enough for terminal guidance tasks in artillery.

5 SIMULATION RESULTS

Simulation results are presented using the nonlinear flight dynamics model (de Celis et al., 2017), where data employed was validated from real flights and model accuracy tested, in order to demonstrate suitability of attitude determination algorithm. A set of ballistic simulated shots was performed as defined in the previous section, in order to compare estimated and simulated attitudes. MATLAB/Simulink R2016a on a desktop computer with a processor of 2.8 Ghz and 8 GB RAM was used.

In order to compare the estimated attitude against real or simulated attitude, the following expressions are represented in Figures 2, 3 and 4: $\phi_{real} - \phi_{estimated}$, $\theta_{real} - \theta_{estimated}$ and $\psi_{real} - \psi_{estimated}$. All these figures represent results for a shot angle of 45° and three different azimuth angles: 0°, 45° and 90°. Note that a larger amount of simulations have been performed, as

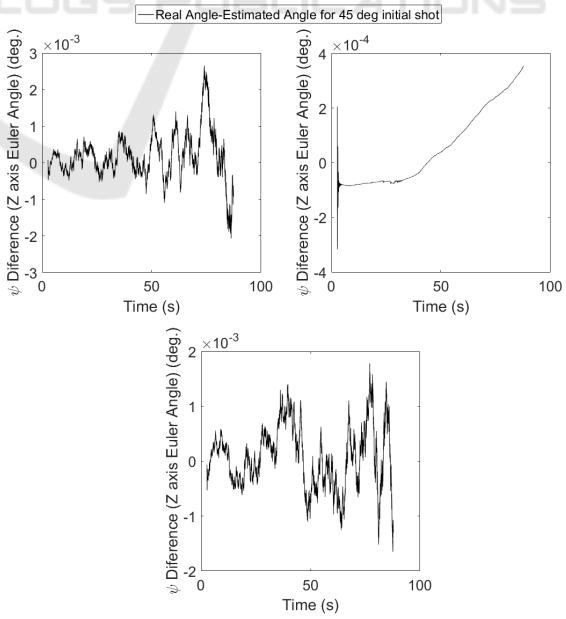

Figure 4: Comparison between estimated and real magnitudes for aircraft yaw angle (ψ) for a shot angle of 45 deg. and azimuths of 0° (left), 45° (right) and 90° (bottom).

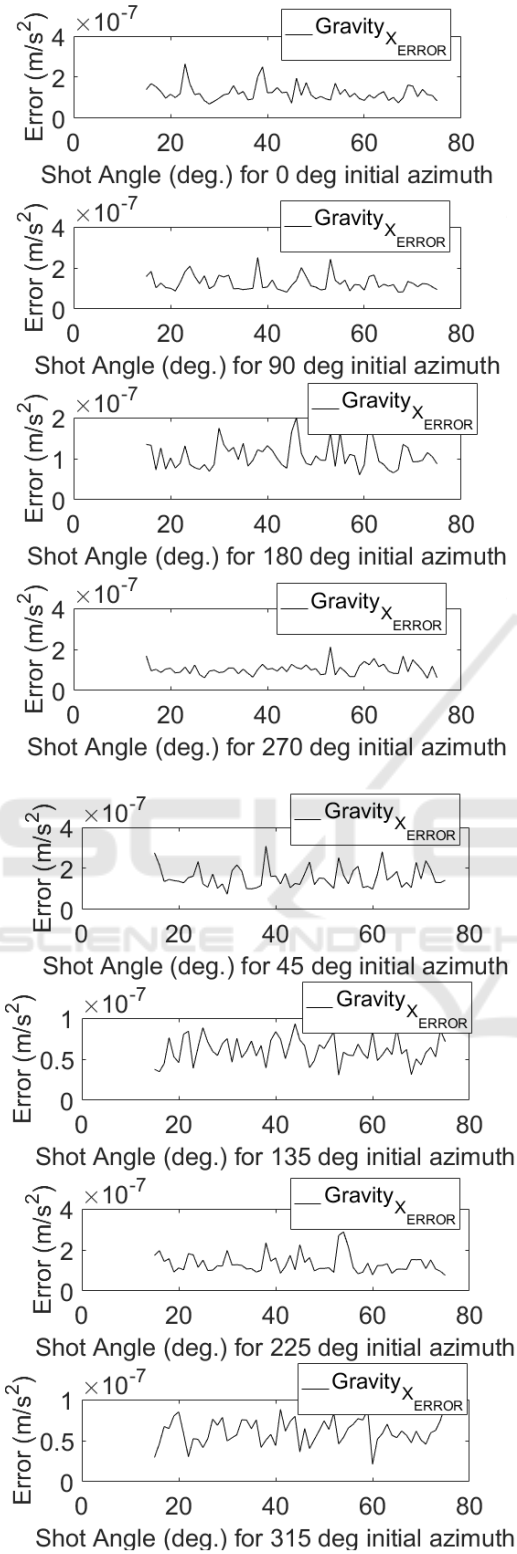

Figure 5: Representation of x_B gravity component Root Mean Squared Error along the whole trajectory for each shot angle and for the 8 azimuths tested.

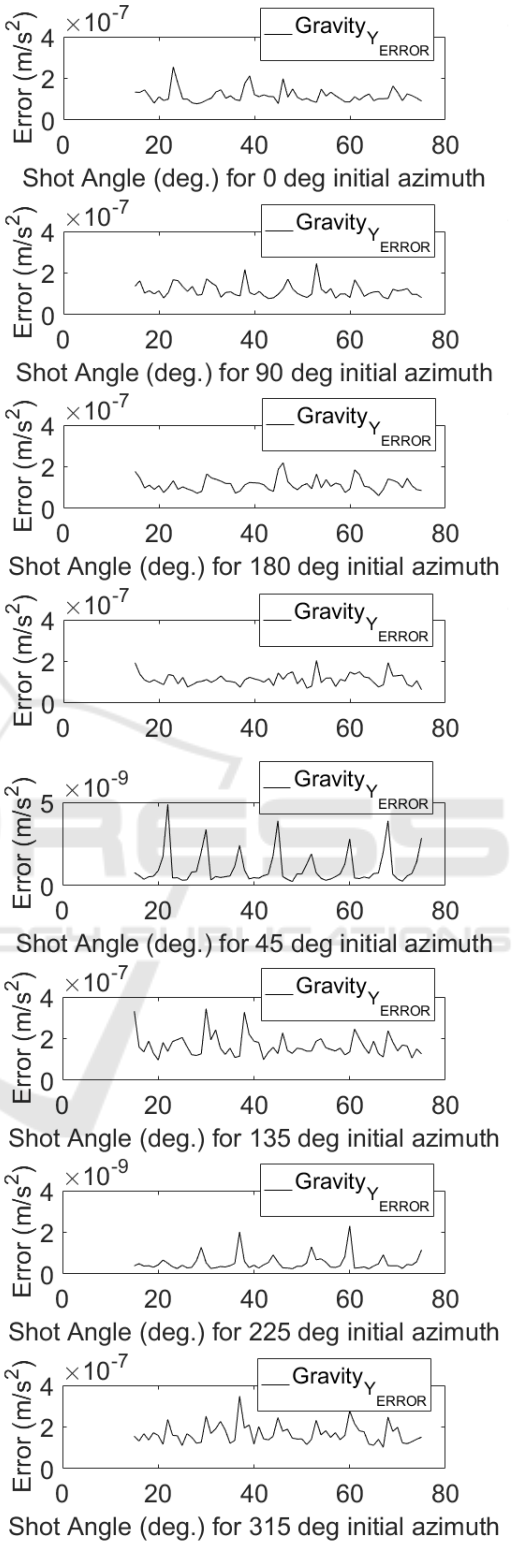

Figure 6: Representation of y_B gravity component Root Mean Squared Error along the whole trajectory for each shot angle and for the 8 azimuths tested.

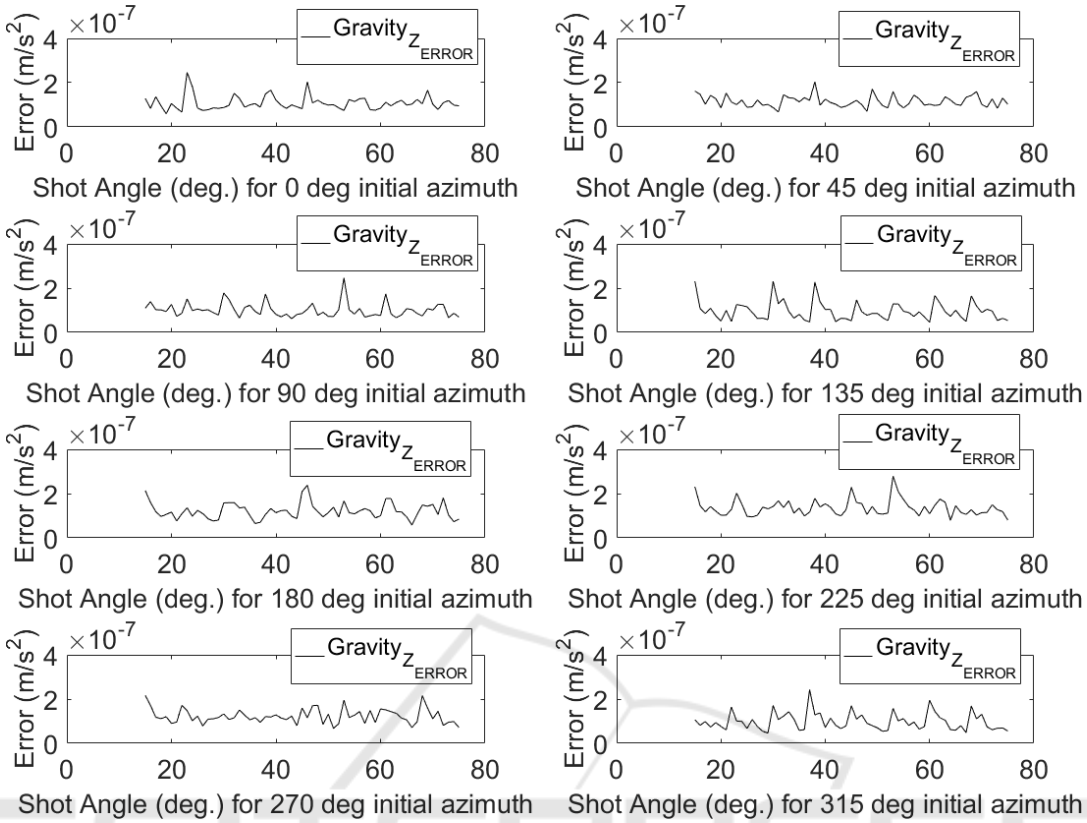

Figure 7: Representation of z_B gravity component Root Mean Squared Error along the whole trajectory for each shot angle and for the 8 azimuths tested.

it was defined previously, but the results are virtually the same.

Note that in the worst of the situations the difference between real and estimated attitude is lower than a magnitude order of 10^{-2}, which assures the applicability of the presented algorithms together with the sensors employed and their associated noises.

In order to quantify the error made in each of the shots along the whole simulated trajectories, the Root Mean Squared Error (RMSE) for each of the 3 Euler angles ($RMSE_{\phi}^{\theta_0,AZ_0}$), ($RMSE_{\theta}^{\theta_0,AZ_0}$) and ($RMSE_{\psi}^{\theta_0,AZ_0}$), and for each of the three components of gravity vector in body axes ($RMSE_{g_{x_B}}^{\theta_0,AZ_0}$), ($RMSE_{g_{y_B}}^{\theta_0,AZ_0}$) and ($RMSE_{g_{z_B}}^{\theta_0,AZ_0}$), are calculated in (28), (29), (30),(31), (32), and (33). These errors depend on the shot launch angle (θ_0) and azimuth (AZ_0).

$$RMSE_{\phi}^{\theta_0,AZ_0} = \sqrt{\frac{\oint(\phi_{real} - \phi_{computed})^2 d\sigma}{\oint d\sigma}} \quad (28)$$

$$RMSE_{\theta}^{\theta_0,AZ_0} = \sqrt{\frac{\oint(\theta_{real} - \theta_{computed})^2 d\sigma}{\oint d\sigma}} \quad (29)$$

$$RMSE_{\psi}^{\theta_0,AZ_0} = \sqrt{\frac{\oint(\psi_{real} - \psi_{computed})^2 d\sigma}{\oint d\sigma}} \quad (30)$$

$$RMSE_{g_{x_B}}^{\theta_0,AZ_0} = \sqrt{\frac{\oint(g_{x_{Breal}} - g_{x_{Bcomputed}})^2 d\sigma}{\oint d\sigma}} \quad (31)$$

$$RMSE_{g_{y_B}}^{\theta_0,AZ_0} = \sqrt{\frac{\oint(g_{y_{Breal}} - g_{y_{Bcomputed}})^2 d\sigma}{\oint d\sigma}} \quad (32)$$

$$RMSE_{g_{z_B}}^{\theta_0,AZ_0} = \sqrt{\frac{\oint(g_{z_{Breal}} - g_{z_{Bcomputed}})^2 d\sigma}{\oint d\sigma}} \quad (33)$$

The computed components of gravity vector, $g_{x_{Bcomputed}}$, $g_{y_{Bcomputed}}$ and $g_{z_{Bcomputed}}$ are obtained in the reality directly from inertial measurement unit sensors, concretely by accelerometers with its associated error. On simulations performed these $g_{x_{Bcomputed}}$, $g_{y_{Bcomputed}}$ and $g_{z_{Bcomputed}}$ are estimated through the following algorithms that take in account previously calculated director cosine matrix on (14) and the errors of accelerometers. The model of gravity vector estimator is described by (34) on where $\overrightarrow{e_{acc}}$ is the error

Table 1: Representation of quadratic errors along the whole trajectory for a set of shot angles and for the 8 azimuths tested and calculation of a representative mean parameter.

		Azimuth AZ_0 (deg)								
Shot Angle (deg.)		0	45	90	135	180	225	270	315	Total
15	$QE_{\phi}^{\theta_0,AZ_0}$	7.69E-07	1.01E-07	1.00E-06	1.93E-06	1.10E-06	3.92E-07	1.30E-06	9.77E-07	3.82E-07
15	$QE_{\theta}^{\theta_0,AZ_0}$	2.32E-04	2.29E-04	2.24E-04	2.21E-04	2.19E-04	2.17E-04	2.12E-04	2.09E-04	7.80E-05
15	$QE_{\psi}^{\theta_0,AZ_0}$	7.69E-06	6.84E-07	6.49E-06	9.87E-06	8.16E-06	9.29E-07	4.58E-06	1.01E-05	2.46E-06
30	$QE_{\phi}^{\theta_0,AZ_0}$	3.24E-06	2.38E-06	1.05E-06	2.33E-06	1.05E-06	3.52E-07	6.13E-07	1.62E-06	6.48E-07
30	$QE_{\theta}^{\theta_0,AZ_0}$	1.46E-04	1.50E-04	2.31E-04	2.28E-04	2.27E-04	2.24E-04	2.21E-04	2.16E-04	7.36E-05
30	$QE_{\psi}^{\theta_0,AZ_0}$	1.44E-05	6.29E-06	7.72E-06	1.25E-05	7.41E-06	1.17E-06	6.60E-06	1.54E-05	3.53E-06
45	$QE_{\phi}^{\theta_0,AZ_0}$	2.45E-06	1.78E-06	2.04E-06	3.91E-06	9.67E-07	3.04E-07	7.51E-07	1.44E-06	7.10E-07
45	$QE_{\theta}^{\theta_0,AZ_0}$	1.40E-04	1.43E-04	1.46E-04	1.50E-04	2.32E-04	2.32E-04	2.28E-04	2.24E-04	6.77E-05
45	$QE_{\psi}^{\theta_0,AZ_0}$	1.10E-05	4.14E-06	1.41E-05	2.08E-05	1.12E-05	9.04E-07	6.63E-06	1.50E-05	4.26E-06
60	$QE_{\phi}^{\theta_0,AZ_0}$	2.55E-06	1.43E-06	1.69E-06	2.05E-06	3.02E-06	2.03E-06	9.50E-07	1.66E-06	7.13E-07
60	$QE_{\theta}^{\theta_0,AZ_0}$	1.36E-04	1.38E-04	1.41E-04	1.43E-04	1.46E-04	1.49E-04	2.34E-04	2.31E-04	5.98E-05
60	$QE_{\psi}^{\theta_0,AZ_0}$	1.14E-05	3.02E-06	1.29E-05	1.67E-05	1.52E-05	5.60E-06	7.26E-06	1.44E-05	4.16E-06
75	$QE_{\phi}^{\theta_0,AZ_0}$	1.46E-06	1.20E-06	1.27E-06	2.56E-06	2.78E-06	1.56E-06	1.66E-06	3.72E-06	7.76E-07
75	$QE_{\theta}^{\theta_0,AZ_0}$	1.33E-04	1.35E-04	1.36E-04	1.38E-04	1.40E-04	1.43E-04	1.46E-04	1.49E-04	4.95E-05
75	$QE_{\psi}^{\theta_0,AZ_0}$	1.10E-05	2.47E-06	9.40E-06	1.45E-05	1.40E-05	4.04E-06	1.46E-05	1.75E-05	4.25E-06
Total	$QE_{\phi}^{\theta_0,AZ_0}$	1.01E-06	7.02E-07	6.55E-07	1.19E-06	8.96E-07	5.27E-07	5.02E-07	9.42E-07	2.95E-07
Total	$QE_{\theta}^{\theta_0,AZ_0}$	7.24E-05	7.29E-05	8.09E-05	8.08E-05	8.81E-05	8.80E-05	9.42E-05	9.29E-05	2.97E-05
Total	$QE_{\psi}^{\theta_0,AZ_0}$	5.05E-06	1.70E-06	4.72E-06	6.85E-06	5.19E-06	1.42E-06	3.87E-06	6.57E-06	1.70E-06

associated to the accelerometer:

$$\begin{bmatrix} g_{x_{Bcomputed}} \\ g_{y_{Bcomputed}} \\ g_{z_{Bcomputed}} \end{bmatrix} = \begin{bmatrix} q_0^2+q_1^2-q_2^2-q_3^2 & 2(q_1q_2+q_0q_3) & 2(q_1q_3-q_0q_2) \\ 2(q_1q_2-q_0q_3) & q_0^2-q_1^2+q_2^2-q_3^2 & 2(q_2q_3+q_0q_1) \\ 2(q_1q_3+q_0q_2) & 2(q_2q_3-q_0q_1) & q_0^2-q_1^2-q_2^2+q_3^2 \end{bmatrix} \cdot \begin{bmatrix} 0 \\ 0 \\ 9.81 \end{bmatrix} + \overrightarrow{e_{acc}} \tag{34}$$

Table 1 shows the Root Mean Squared Errors for the 3 Euler angles for different shot angles and azimuths. The first column shows the shot angle and the second one the displayed error ($RMSE_{\phi}^{\theta_0,AZ_0}$), ($RMSE_{\theta}^{\theta_0,AZ_0}$ and $RMSE_{\psi}^{\theta_0,AZ_0}$). The rest of the columns show the numerical values of the errors for different azimuths. Finally right column named total, represents the Root Mean Squared Errors for the set of azimuths represented on the same row. Equally the last three rows represent the Root Mean Squared Errors for the set of shot angles represented on the same column. Finally the three values of the bottom-right corner can be considered as an estimation of the whole error of the attitude calculation algorithms.

Figures 5, 6 and 7 show the following Root Mean Squared Errors: $RMSE_{g_{x_B}}^{\theta_0,AZ_0}$, $RMSE_{g_{y_B}}^{\theta_0,AZ_0}$ and $RMSE_{g_{z_B}}^{\theta_0,AZ_0}$ along the whole trajectory for each shot angle and for the 8 azimuths.

Note that the obtained Root Mean Squared Errors for all the measures of interest presented in this paper are small enough to consider the proposed algorithm for estimating attitude of high dynamic vehicles at a low cost. Comparison between real aircraft attitude, which can be assumed near to the attitude provided by a precise gyroscope, and the attitude obtained by exposed algorithms, never differ from 10^{-3} degrees, which is a very accurate value for most of the projectile applications.

6 CONCLUSIONS

A novel low-cost approach for estimating attitude of aerial platforms has been proposed. This approach is based on the measurement of two different vectors: speed and gravity vector. They are measured in two different reference frames using a GNSS sensor and a set of accelerometers. The presented algorithm is of special interest for high dynamic vehicles where other low-cost approaches, such as the ones using magnetometers, are not suitable.

Nonlinear simulations based on ballistic rocket launches are performed to obtain ideal attitude and compare it to the attitude obtained by the proposed approach. Computational results show that errors made are small enough to consider the presented algorithm as a good candidate for using it within a control algorithm. Note that the low-cost needed components make this approach highly interesting for non-re-usable vehicles.

REFERENCES

Crassidis, J. L., Markley, F. L., and Cheng, Y. (2007). Survey of nonlinear attitude estimation methods. *Journal of guidance, control, and dynamics*, 30(1):12–28.

de Celis, R., Cadarso, L., and Sánchez, J. (2017). Guidance and control for high dynamic rotating artillery rockets. *Aerospace Science and Technology*. http://dx.doi.org/10.1016/j.ast.2017.01.026.

Eure, K. W., Quach, C. C., Vazquez, S. L., Hogge, E. F., and Hill, B. L. (2013). An application of uav attitude estimation using a low-cost inertial navigation system. *NASA/TM2013-218144*. https://ntrs.nasa.gov/archive/nasa/casi.ntrs.nasa.gov/20140002398.pdf.

Gebre-Egziabher, D., Elkaim, G. H., Powell, J., and Parkinson, B. W. (2000). A gyro-free quaternion-based attitude determination system suitable for implementation using low cost sensors. In *Position Location and Navigation Symposium, IEEE 2000*, pages 185–192. IEEE.

Gebre-Egziabher, D., Hayward, R. C., and Powell, J. D. (1998). A low-cost gps/inertial attitude heading reference system (ahrs) for general aviation applications. In *Position Location and Navigation Symposium, IEEE 1998*, pages 518–525. IEEE.

Henkel, P. and Iafrancesco, M. (2014). Tightly coupled position and attitude determination with two low-cost gnss receivers. In *Wireless Communications Systems (ISWCS), 2014 11th International Symposium on*, pages 895–900. IEEE.

Ismail, A., Ashraf, K., Metawea, A., Mostfa, I., Saeed, A., Helal, E., Essawy, M., Abdelazim, M., Ibrahim, M., Raafat, R., et al. (2015). A high-performance self-clocked digital-output quartz gyroscope. In *SENSORS, 2015 IEEE*, pages 1–4. IEEE.

Kuipers, J. B. et al. (1999). *Quaternions and rotation sequences*, volume 66. Princeton university press Princeton.

Ma, D.-M., Shiau, J.-K., Wang, I., Lin, Y.-H., et al. (2011). Attitude determination using a mems-based flight information measurement unit. *Sensors*, 12(1):1–23.

Mizell, D. (2003). Using gravity to estimate accelerometer orientation. In *Proc. 7th IEEE Int. Symposium on Wearable Computers (ISWC 2003)*, volume 252. Citeseer.

Savage, P. G. (2000). *Strapdown analytics*, volume 2. Strapdown Associates Maple Plain, MN.

Springmann, J. C. and Cutler, J. W. (2014). Flight results of a low-cost attitude determination system. *Acta Astronautica*, 99:201–214.

Yun, X., Bachmann, E. R., and McGhee, R. B. (2008). A simplified quaternion-based algorithm for orientation estimation from earth gravity and magnetic field measurements. *IEEE Transactions on instrumentation and measurement*, 57(3):638–650.